EVOH/Clay Nanocomposites Produced by Melt Processing

N. ARTZI, Y. NIR, D. WANG, *and* M. NARKIS*

Department of Chemical Engineering

and

A. SIEGMANN

Department of Materials Engineering
Technion - Israel Institute of Technology
Haifa 32000, Israel

Ethylene-vinyl alcohol copolymer (EVOH)/clay nanocomposites were prepared via a dynamic melt-intercalation process. The phase morphology and the crystallization behavior of the nanocomposites were investigated, using DSC, DMTA, XRD and SEM. It was found that the treated clay content and dynamic processing time affect the viscosity of the EVOH/clay mixtures: higher clay contents and longer mixing times result in higher torque/viscosity levels. This is due to the increased interaction of the molten polar matrix (EVOH) with the treated organosilicate surface. Under the dynamic high shearing forces, the polymer penetrates the clay agglomerates/aggregates, intercalates within the organoclay galleries, and finally causes delamination. Thermal analysis of the EVOH/clay nanocomposites showed that the melting temperature, crystallization temperature and heat of fusion of the EVOH matrix, sharply decrease with increasing both, the clay content and processing time. The intercalation level was characterized by X-ray diffraction (XRD), which verified an increased gallery height. The DMTA spectra showed that longer processing times resulted in higher damping (E" intensity) levels of the EVOH/clay composites, indicating higher fractions of the EVOH amorphous phase. However, no T_g changes were seen in spite of the high polymer/treated clay interaction levels, which may be attributed to a plasticizing effect of the low molecular weight organic cations.

INTRODUCTION

Polymer melt intercalation is a promising new approach to fabricate polymer-layered silicate nanocomposites, apparently by using a conventional melt-mixing technology. The absence of solvents makes the direct intercalation an environmentally sound and economically advantageous method (1). A strong interaction of the silicates with the polymer matrix, attained by compatibilization of the layered silicate with prudent chosen intercalants, leads to polymer melt penetration into the silicate galleries, i.e., to melt intercalation. As polymer-silicate interactions become stronger and intercalation progresses, the gallery height increases, and under the dynamic process, exfoliation may take place. The intercalation followed by delamination processes lead to dispersion of nano-scale thick clay platelets. Such systems exhibit improved modulus and strength, practically without affecting the impact resistance, as is usually the case for conventional filled polymers. Also, quite often the thermal stability, e.g. heat distortion temperature (HDT), increases. The dispersed clay platelets may strongly affect permeability by dictating a tortuous pathway for permeant molecules transversing through the nanocomposite. The combined enhanced barrier characteristics, chemical resistance, reduced solvent uptake and flame retardancy of clay-polymer nanocomposites all benefit from the hindered diffusion pathways through the nanocomposite.

In recent years, numerous research works were reported in the field of clay-nanocomposites, using such polymers as nylon 6, polypropylene and polystyrene as matrices, and DSC, XRD, TEM and other methods

*To whom correspondence should be addressed.

for characterization (2–14). These studies have shown higher matrix melting temperatures (Tm), crystallization temperatures (Tc) and enthalpy values, compared to the neat matrices, without any DSC evidence for the existence of a glass transition temperature (T_g). The present study focuses on preparation under dynamic conditions and characterization of EVOH/clay nanocomposites. The relationships between intercalation level (by X-ray diffraction) and melt viscosity (mixing torque), thermal behavior, and dynamic-mechanical behavior of the nanocomposites were studied.

EXPERIMENTAL

Materials

The EVOH (ethylene vinyl alcohol copolymer) used in this study is a commercial product, Kuraray, of Japan, consisting of 32 mole % ethylene. The treated clay used (Nanomer-1.30E, an onium ion surface modified montmorillonite mineral) and the reference untreated clay were obtained from Nanocor, of Illinois. The treated organo-clay contains 70–75 wt% montmorillonite and 20–25 wt% octadecylamine. It is claimed to be designed for ease of dispersion into amine-cured epoxy resins to form nanocomposites.

Preparation Methods

Prior to melt blending, the EVOH copolymer was milled into a powder. The polymer and clay powders were dried in a vacuum oven at 80°C and 60°C, respectively, for 15 hrs. The components were dry-blended at selected ratios, and subsequently melt-mixed at several temperatures (210°C, 220°C and 230°C) at 60 rpm, in a Brabender plastograph, equipped with a 50 cm^3 cell at different mixing times (10 and 45 minutes). The melt-mixing step was performed also in a Haake Rheocord 90 mixer (Haake GmbH, Germany) at 230°C, at 60 and 150 rpm. All the resulting blends were compression molded at 230°C to obtain 3 mm thick plaques.

Characterization

The phase morphology of the blends was studied by electron microscopy. A Jeol JSM 5400 scanning electron microscope (SEM) was employed for observation of freeze-fractured and microtomed surfaces. All samples were gold sputtered prior to observation. The dynamic mechanical properties of the compression molded samples were measured by a dynamic mechanical thermal analysis system (DMTA, Perkin Elmer Series 7), in the three-point bending mode. The frequency used was 1 Hz., and heating was carried out under an inert nitrogen atmosphere at a rate of 3°C/min. Differential scanning calorimetry (DSC) was employed for characterizing the thermal behavior of the composites. A Mettler DSC 30 system, under an inert nitrogen atmosphere, at a heating rate of 10°C/min was used. Samples were heated to a temperature above their melting, cooled at the same rate, and subsequently reheated. The melting behavior was determined from the second heating run. The layered structure of the clay was examined by a D/Max 2400, X-ray diffractometer (XRD), with a CuKα radiation operated at 40kV, 100mA and a scanning rate of 2°/min.

RESULTS AND DISCUSSION

Melt-mixing

Intercalation and/or delamination of clay in the presence of EVOH (ethylene vinyl alcohol copolymer), can be accomplished by melt-mixing in a Brabender Plastograph. *Figures 1–3* show the mixing torque as a function of mixing time for the following blends: 85/15 EVOH/clay, for two types of clay, namely, treated (1.30E) and untreated (*Fig. 1*), 85/15 EVOH/clay (1.30E) at two different mixing temperatures (*Fig. 2*), and EVOH/clay (1.30E) for different treated clay contents (*Fig. 3*). Under the dynamic mixing conditions, the gradual viscosity increase reflects on the fracturing of the organoclay particles into small aggregates and also between lamina, followed by a delamination process, eventually leading to blending of thin platelets into the EVOH matrix. Under static "blending" conditions, i.e., prolonged heating without shearing, intercalation is the dominant step (15–17). However, under dynamic conditions, delamination, in addition to intercalation, may be a major step, with a suggested onion-like delamination characteristic behavior for highly interacting clay/matrix systems.

Figure 1 shows that the viscosity of the composite with the untreated clay is almost constant, implying that the clay particles stay practically intact, behaving as regular filler particles. However, the viscosity of the system with treated clay rises due to fracturing processes, formation of new surfaces and additional interaction with the EVOH matrix. Filler agglomeration/deagglomeration processes may also play a role on the level of the required mixing power (torque), where the matrix character and interaction level are important parameters (18). The blending temperature is an important parameter in the structuring process (*Fig. 2*). At the higher temperature (230°C compared to 210°C), despite the polymer viscosity decrease, the torque rise is higher, presumably owing to the build-up of higher interaction levels accompanied by fracturing and delamination processes. Such polymer/clay interactions partially arrest polymer segmental movements, as was suggested by Giannelis *et al.* (1), resulting in a rubber-like elastic behavior.

The clay content also plays an important role in determining the delamination process (*Fig. 3*). At higher clay contents, the torque rise is more pronounced, owing to the formation of more interaction sites, which reduce the segmental movements level, and to the enhanced platelets peeling, contributing to the sharp increase of the torque/viscosity with time. When a network of continuous platelets is established, flow mechanisms such as plug flow, slip at the wall phenomena, and even mechanical fracturing of the hot mass in the mixing cell are taking place (19). *Figure 3* also shows that the heat stability level of the neat

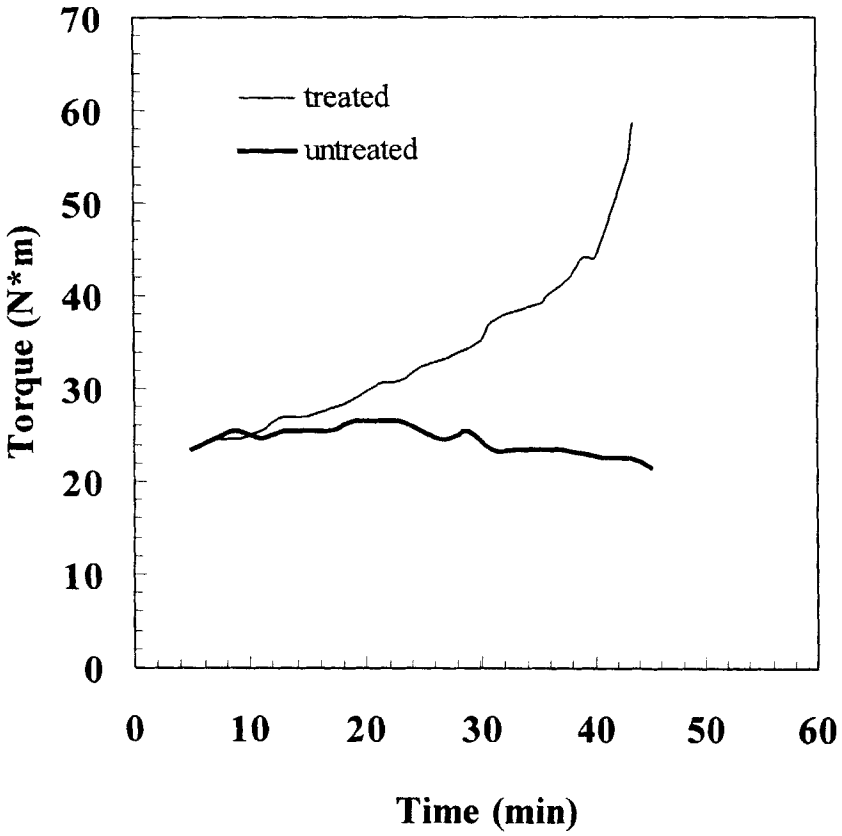

Fig. 1. Brabender plastograms of 85/15 EVOH/clay blends at 230°C, and 60 rpm.

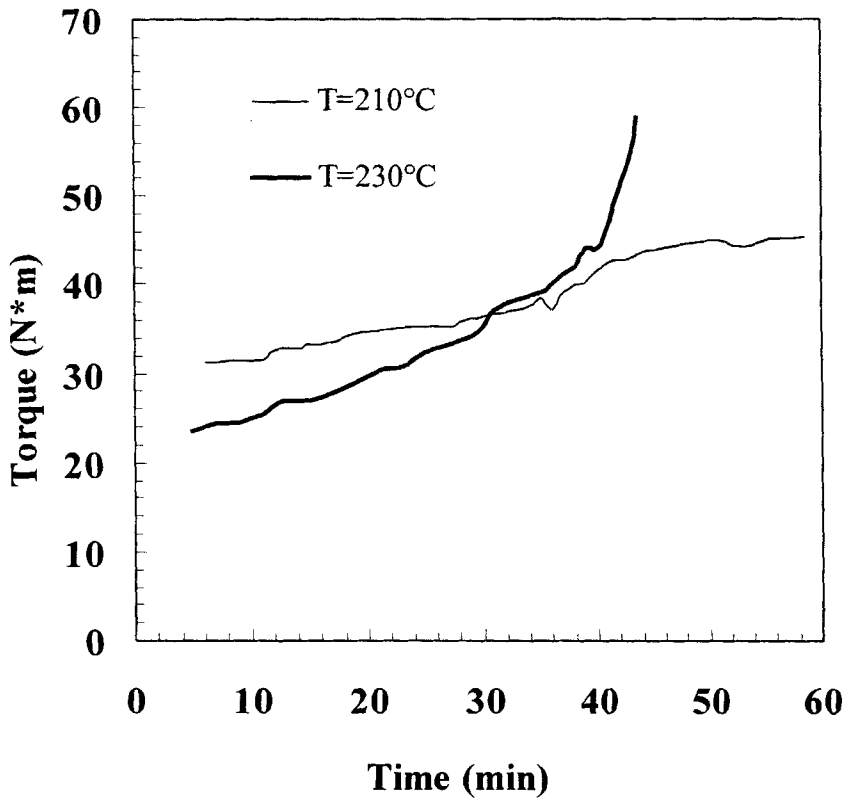

Fig. 2. Brabender plastograms of 85/15 EVOH/treated clay blends at various temperatures, and 60 rpm.

EVOH copolymer is significant and sufficient for reliably studying the dynamic melt mixing of the EVOH/clay composites.

The effect of the combination of high temperature and high rotation speed (150 rpm compared to 60 rpm), experienced in the Haake machine, is demonstrated in *Fig. 4*. An interpretation of this behavior is that when the separately dispersed platelets reach a certain concentration, presumably when continuity of platelets is approached and gel-like behavior becomes important, a dramatic viscosity increase occurs. The temperature, set to 230°C, has actually reached 280°C, near the maximum torque level seen in *Fig. 4*. The torque rise already became pronounced after 3 min of mixing, presumably at the beginning of formation of continuity of platelets, and the maximum torque level occurred soon thereafter at 5.5 min. The material's rigidity is increasing because of the increasing level of EVOH/clay interaction, thus eliminating segments and chains from the flowing polymer melt. The sharp torque decrease (*Fig. 4*) is a result of mechanical degradation of the hot mass under the dynamic mixing conditions, which occurs when the system flowability decreases, attaining a certain low level. At this point the material is undergoing milling into a powder, in the hot mixing cell. A similar torque behavior was reported for a different system gradually losing its flow properties, i.e., polyethylene undergoing crosslinking reactions in a dynamic melt mixing process (Brabender cell), in the presence of high-temperature decomposing peroxides (20). In these experiments the polyethylene melt was ground in the Brabender mixing cell into a powder of crosslinked polyethylene particles, accompanied by a dramatically decreasing torque.

In summary, in highly interacting systems, in addition to a fracturing process of the clay particles, an onion-like delamination process is suggested, as schematically illustrated in *Fig. 5*. External platelets are subjected to dynamic high shear forces, which ultimately cause their delamination from the stack of layers building the original clay particle. The effect of interaction level on the shearing efficiency in a dynamic melt mixing process was previously demonstrated by the authors in polyaniline/polymer melts (21). In such systems, very fine polyaniline particles form by fracturing of large polyaniline aggregates in these highly interacting systems (i.e., polyaniline/polyamide), contrary to low level interacting systems (polyaniline/polyethylene), where low fracturing levels are obtained. Accordingly, processing of highly interacting systems in an efficient shearing field is an important parameter in the fracturing and delamination steps of clays, leading to formation of nanocomposite structures.

DSC

Differential scanning calorimetry (DSC) studies offer further support to the high interaction level in the EVOH/clay system. *Figure 6* shows the second DSC run of the neat EVOH that was melt-mixed for 45 min, and for the 85/15 EVOH/treated clay blend at two mixing times, 10 and 45 min. As seen, the interaction level achieved in the dynamic process affects the thermal behavior. Chains attached to the platelets are partially hindered from taking part in the flow process and their crystallization process is also hindered. Thus, the platelets affecting the crystallization process are both those in the intercalated particles and those already dispersed. Thus, the compound that was melt-mixed for 10 min shows a T_m of 178.9°C, similar to the neat EVOH (179.6°C), but a lower enthalpy value, 72.2mJ/g (normalized to EVOH content), compared to 82.7mJ/g for the neat EVOH. After 45 min of mixing, much lower melting temperature and enthalpy values, 159.5°C and 55.5mJ/g respectively, are found (*Fig. 6*). These results differ from reports on other systems (7, 15, 16, 22, 23). The crystallization process in the presence of clay particles, especially clay nano-platelets, generates smaller EVOH crystals, having a lower melting temperature. Probably, the clay plays a role of a "low quality nucleating agent," which in addition hinders the crystallization process, owing to its high interaction level with EVOH. The literature reports on an opposite crystallization behavior, i.e., a higher crystallization rate for a PET/clay system (compared to the neat PET) (24). Presumably, owing to the much lower interaction level in the PET/clay system, the clay does not interrupt the crystallization process. The melting peak of the clay containing EVOH is broadened at the longer processing time (*Fig. 6*). The presence of a higher clay content, as in *Fig. 7* (15% versus 5%), and the long processing time, 45 min, also result in reduction of T_m and enthalpy values relative to the neat EVOH. Since, in the presence of higher content of clay platelets, the crystallization process is more hindered, for long processing times a reduction in T_c occurs, i.e., a higher cooling degree is required, as shown in *Fig. 8*.

XRD

X-ray diffraction is a conventional method to characterize the gallery height in clay particles. As the intercalation process progresses, the gallery height increases, resulting in a shift of characteristic reflections to lower angles. *Figure 9* depicts X-ray diffraction patterns for the neat EVOH, treated clay and the composites of 85/15 EVOH/treated clay, which were processed for 10 and 45 min at 230°C. The basal reflections, characteristic of the virgin treated clay (2θ = 3.58°, 8.12°; $d_{(001)}$ = 2.46 nm), and the neat polymer (2θ = 10.78°, 20.1°, 21.24°) are included in the diffraction pattern. As a result of the melt-mixing process, for the EVOH/treated clay system, the characteristic peaks of the treated clay shift to lower degrees (2θ = 2.7°, 5.5°, 8.34°; $d_{(001)}$ = 3.26 nm) and (2θ = 2.72°, 5.42°, 8.12°; $d_{(001)}$ = 3.25 nm) for 10 and 45 min, respectively, which is attributed to intercalation. Namely, a 10 min processing duration is a sufficient time for intercalation to occur. Further mixing may

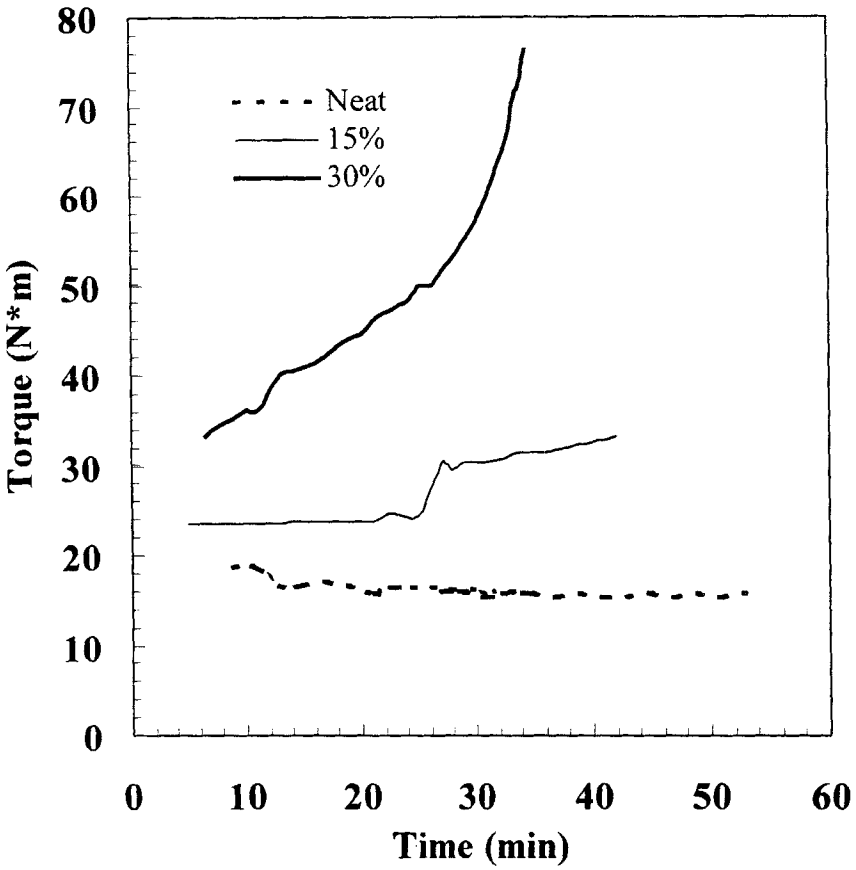

Fig. 3. Brabender plastograms of EVOH containing different amounts of treated clay at 220°C, and 60 rpm.

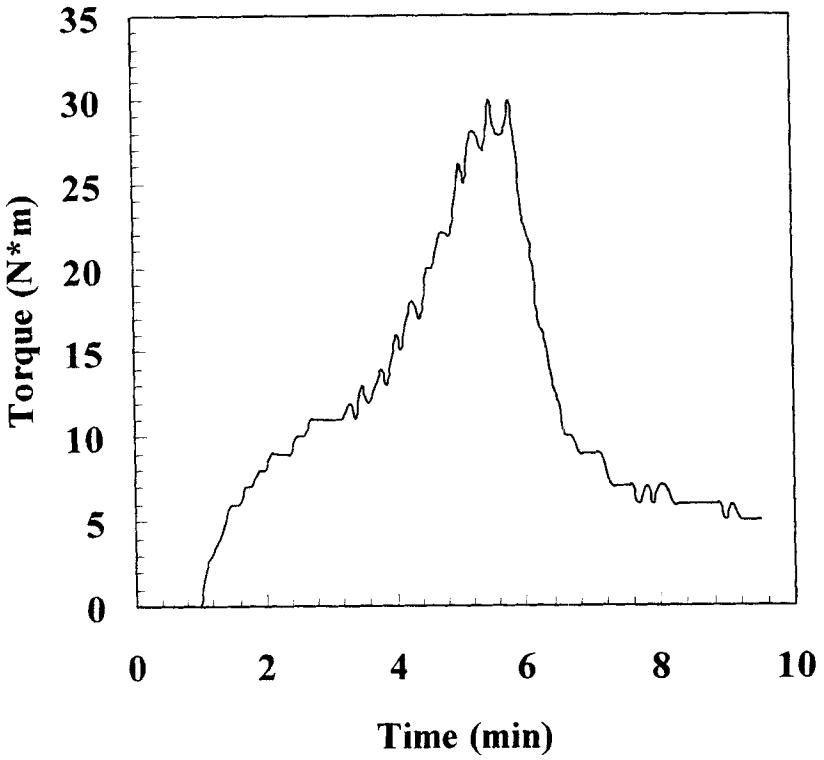

Fig. 4. Haake plastogram of a 85/15 EVOH/treated clay blend at 230°C and 150 rpm.

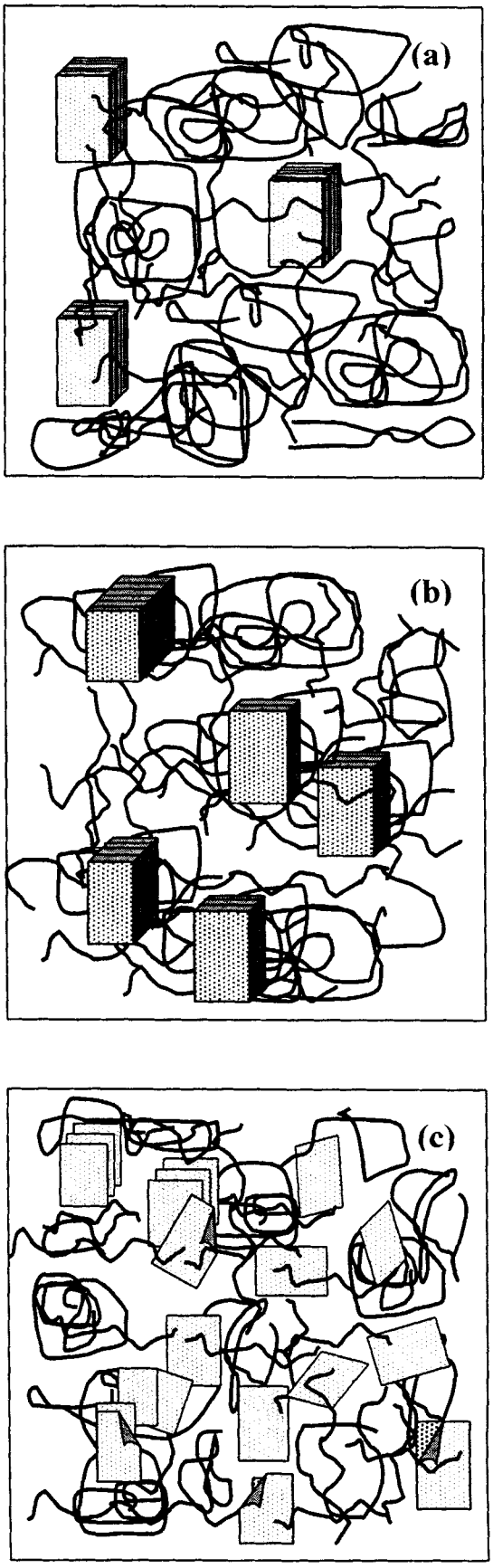

Fig. 5. Schematic description of clay fracturing and an onion-like delamination process, where thin platelets peel off and blend into the matrix: (a) before intercalation and/or delamination process. (b) intercalation and clay fracturing. (3) advanced delamination process.

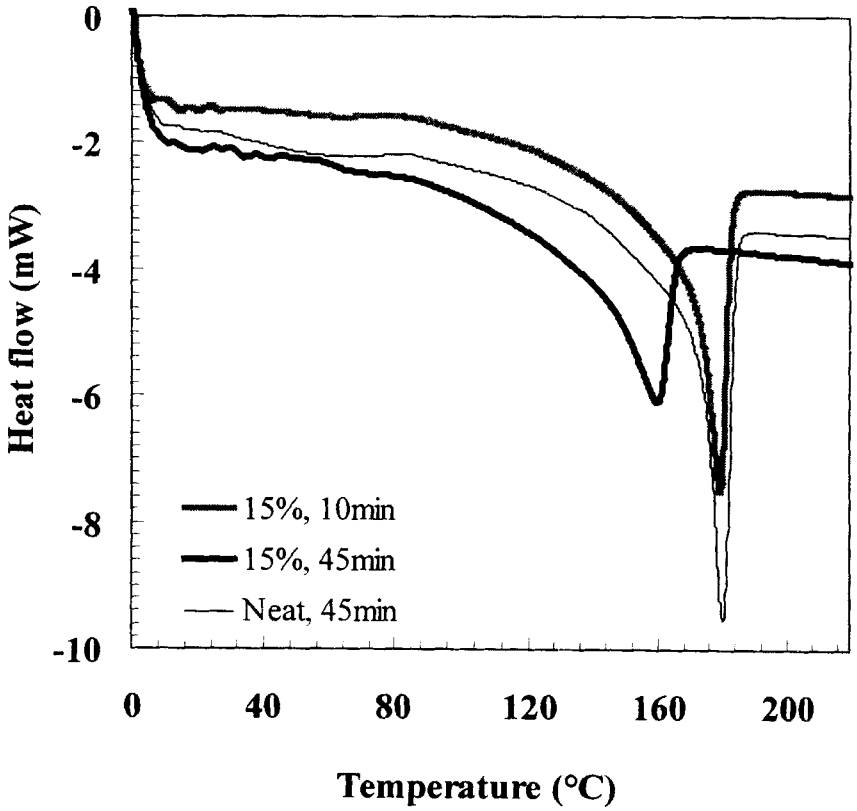

Fig. 6. DSC second heating thermograms of neat EVOH and 85/15 EVOH/treated clay composites prepared at different processing times, at 230°C.

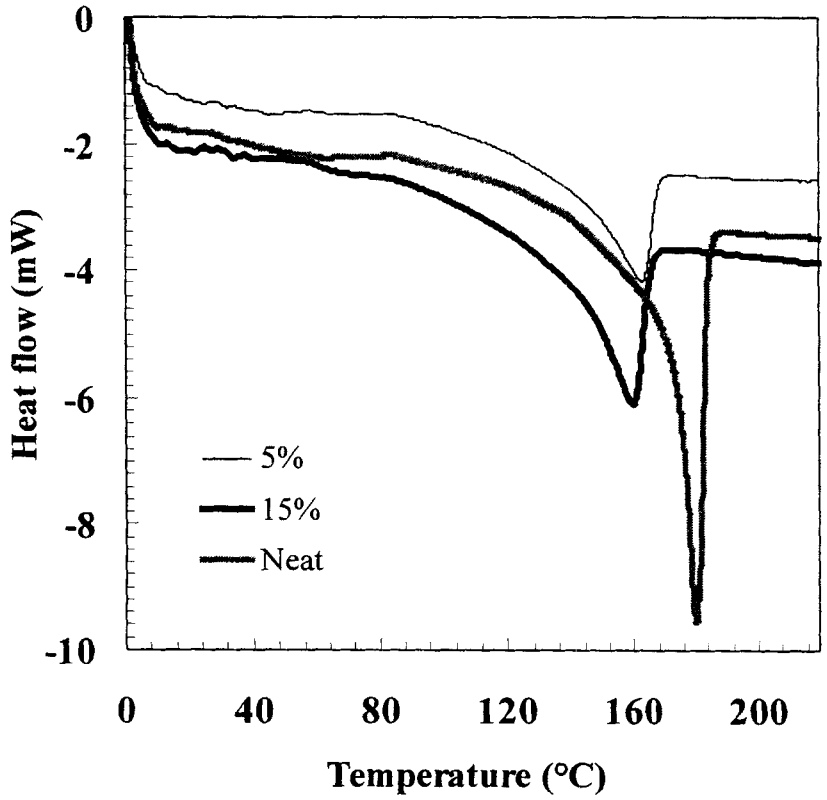

Fig. 7. DSC second heating thermograms of neat EVOH and EVOH/treated clay composites containing different amounts of clay prepared by 45 min of mixing in the Brabender cell, at 230°C.

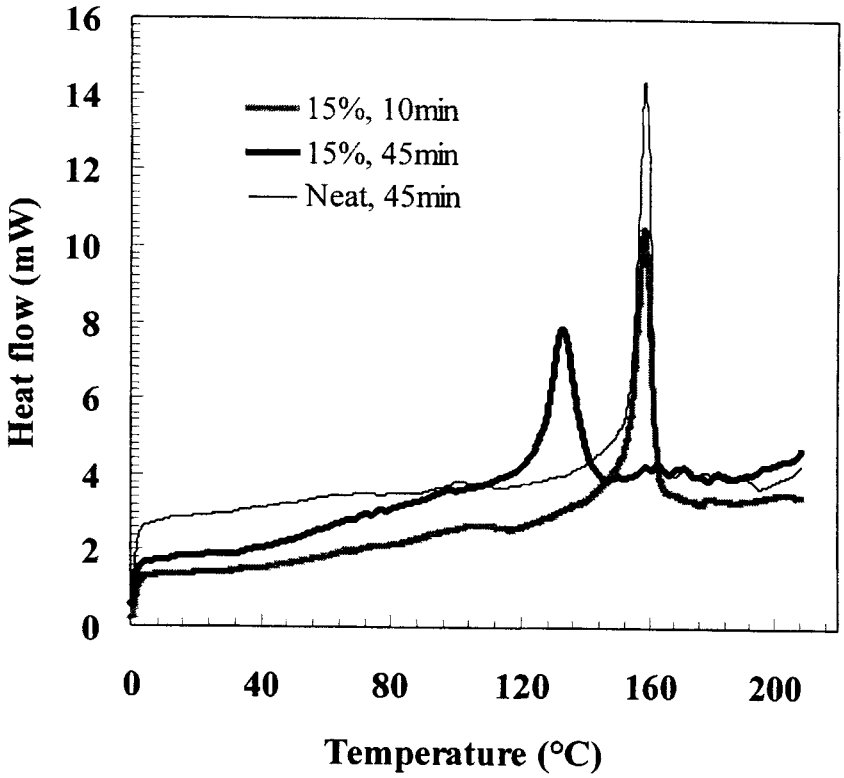

Fig. 8. DSC cooling thermograms of neat EVOH and 85/15 EVOH/treated clay composites prepared at different processing times, at 230°C.

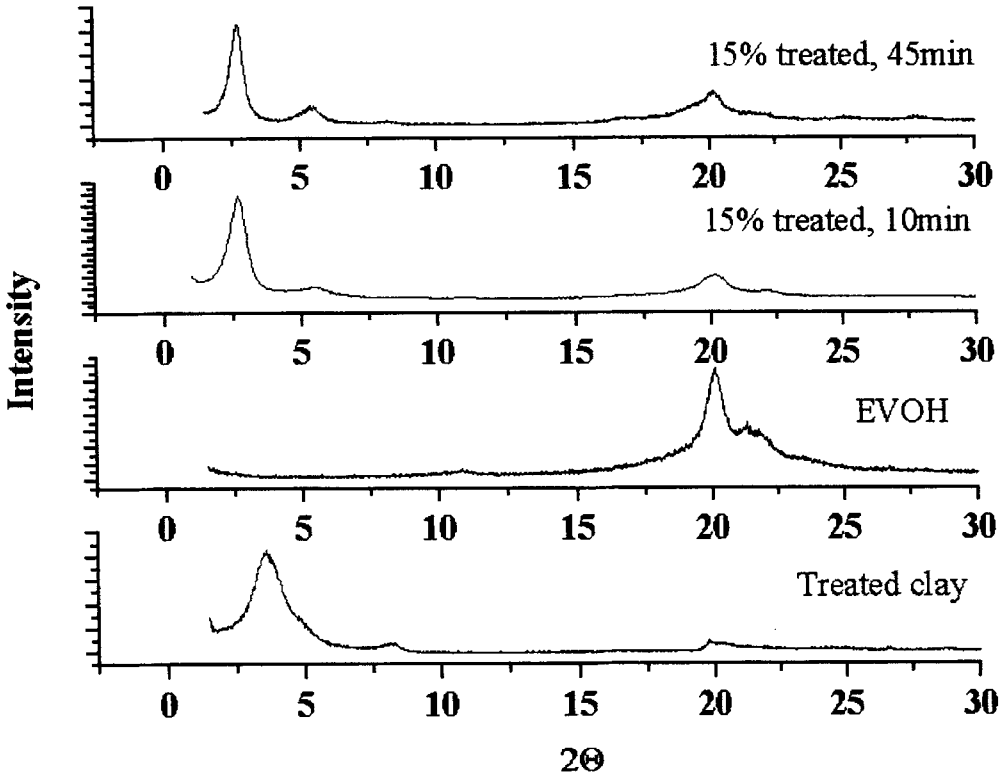

Fig. 9. X-ray diffraction patterns of neat clay, neat EVOH and 85/15 EVOH/treated clay blend, prepared by 10 and 45 min of mixing in the Brabender cell, at 230°C.

thus lead to a better dispersion of the already intercalated clay. The width of peaks (measured by the full width at half maximum) is inversely proportional to the coherence length of scattering entities, and therefore reflects the coherent order of the silicate layers. The breadth of the (001) reflection for the intercalated treated clay is, interestingly, even narrower than that of the unintercalated treated clay, pointing out to an ordered intercalate. Further information about the order level in the system can be obtained from the reflection orders obtained using the Bragg law. Using the d-spacing of the intercalated treated clay that was melt-mixed for 45 min as an example, ($d_{(001)}$ = 3.25 nm), to calculate the angles of higher order reflections results in similar experimental (2θ = 5.42°, 8.12°) and calculated values (2θ = 5.44°, 8.17°, for n = 2, 3, respectively). It should be mentioned that the peak at 2θ = 8.12° can be also related to residues of the original treated clay. However, the higher order proposition is preferred, since in the diffraction pattern of blends with higher clay content, the intensity of this peak is not higher. Comparison of the EVOH characteristic peaks at 2θ = 20.1° and 2θ = 21.2°, for the neat EVOH and the 85/15 EVOH/clay blend, which was melt-mixed for 45 min at 230°C, provides further evidence for the significant decrease in the EVOH crystallinity as previously discussed. The rise in the amorphous phase content is presumably a contribution of both EVOH adsorbed onto the clay surfaces and EVOH within the clay particles and galleries. In both cases, the crystallization process has not been completed, owing to the high EVOH interaction level with the clay.

DMTA

Figure 10 depicts the loss modulus curves of neat EVOH, 85/15 EVOH/untreated clay processed at 230°C for 45 min and 85/15 EVOH/treated clay processed at 230°C for 10 and 45 min. The EVOH/ treated clay composites show an α-transition peak at approximately 50°C, similar to the neat EVOH (at 1 Hz). It should be recalled that a glass transition was not detected in DSC thermograms, similar to the literature reports (1, 7, 15, 23, 25). The significance of the mixing time, 10 and 45 min, is demonstrated in the figure for the treated clay. One can expect two opposing effects on the α transition: the confined chain mobility owing to interaction buildup, and an increased mobility due to reduction in the crystallinity degree as a consequence of the polymer/clay interaction. Since the decrease in the melting enthalpy value is more pronounced for the compound that was melt-mixed for 45 min, it is suggested that the former effect (reduced mobility) is more dominant for the 10 min mixing compound and the latter effect (increased mobility) is more dominant for the 45 min compound. The damping rise can also be related to the development of additional interfaces between the matrix and the

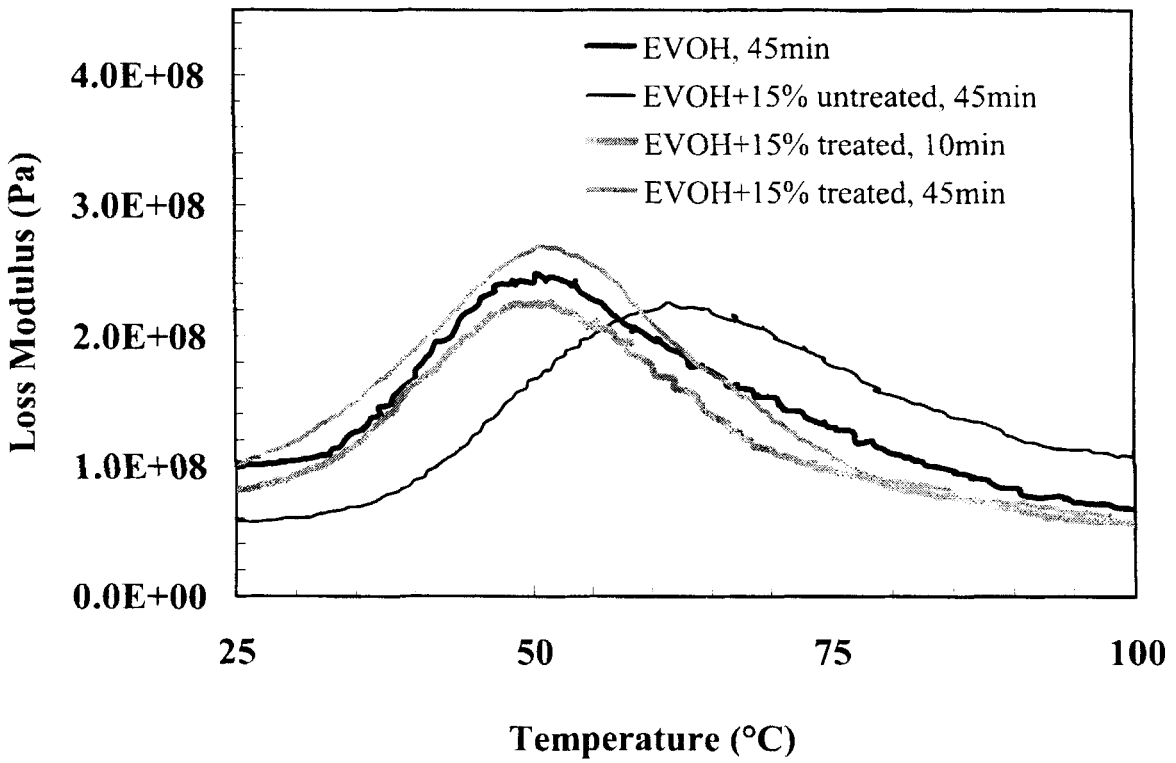

Fig. 10. E'' (loss modulus) of neat EVOH, 85/15 EVOH/untreated clay blend, 45 min mixing in the Brabender cell and 85/15 EVOH/treated clay blends, prepared by 10 min and 45 min mixing in the Brabender cell, at 230°C.

numerous clay particles, formed after 45 min in the Brabender mixing cell. This phenomenon is the cause for more interphase and interparticle friction, increasing the magnitude of the loss peak. The untreated clay apparently behaves as a conventional platy filler, which normally causes a slight T_g increase and a damping decrease (26–28). The 12°C T_g increase, however, is significant and reflects a relatively high interaction level generated during the long high temperature mixing time. This phenomenon does not take place with the treated clay. Presumably, the low molecular weight organic cations in the treated clay function as plasticizers, decreasing T_g, as recently reported (29).

SEM

SEM studies offer further support for the intercalation progression and delamination processes for the longer mixing times. Observation of the clay dispersion within the polymer matrix by SEM was first performed on cryogenically fractured surfaces (*Figs. 11a* and *11b*). EVOH/clay fractured surfaces are difficult to study, because of the developed structure observed for the neat EVOH. Furthermore, as a result of the EVOH/clay high interaction levels, it is difficult to distinguish between the two phases. However, microtomed surfaces (*Figs. 11c* and *11d*) provide more coherent pictures. Microtomed samples of neat EVOH exhibit a

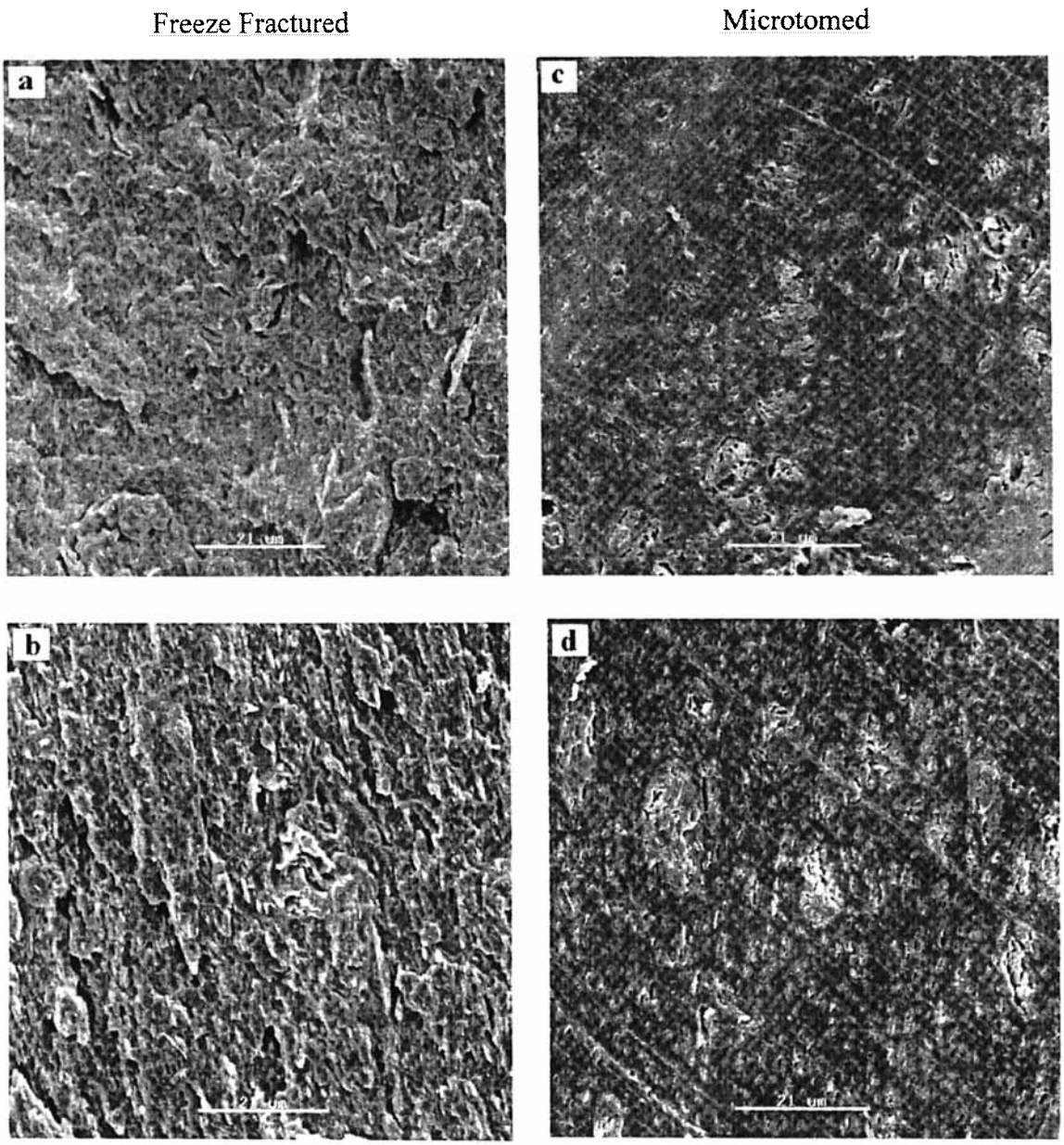

Fig. 11. SEM micrographs of fractured surfaces 85/15 EVOH/treated clay blends prepared by mixing in the Brabender cell, at 230°C, for (a) 10 min freeze-fractured, (b) 45 min freeze-fractured, (c) 10 min microtomed, and (d) 45 min microtomed.

quite smooth surface area, and therefore, observed foreign particles can be related to the clay phase. The clay particles dispersed in the EVOH matrix are distinguishable in these microtomed micrographs. The observed elongated shaped voids represent clay particles that have been pulled out by microtoming. *Figures 11a,c* and *11b,d* depict blends that were melt-mixed in the Brabender for 10 and 45 min, respectively. Both composites were compression molded at 230°C, 50 atm, for 15 min. The two composites (two different mixing times) show different morphologies. The compound processed for 45 min has a more complex morphology, and the fracture surfaces show considerable surface roughness (*Fig. 11b* compared to *Fig. 11a*). The microtomed surfaces show many more clay particles after 45 min of mixing (*Fig. 11d* compared to *Fig. 11c*). This is probably due to fracturing of the micron-scale clay aggregates in the Brabender cell. The fracturing process may eventually lead to dispersed platelets in the continuous matrix, namely a delamination process, without a preceding intercalation step. There is a wide distribution of the clay particles size, ranging from 10μ to less than 1μ, however, a smaller particle size is beyond the SEM resolution.

CONCLUSIONS

Dynamic melt-mixing of EVOH/treated organo-clay mixtures is accompanied by a significant torque increase owing to clay particle fracturing, intercalation and delamination processes and the buildup of significant levels of polymer/clay interaction. Contrary to the organo-clay, the untreated pristine clay is acting as a regular filler. Whereas in static blending, intercalation may be the dominant step, in dynamic melt blending, delamination (exfoliation) may be the major step.

In the EVOH/clay system, both Tm and Tc of the EVOH significantly decrease, by increasing the clay content and melt processing time. The DMTA spectra showed that longer processing times resulted in higher damping (E" intensity) levels of the EVOH/clay composites. However, no T_g changes were seen in spite of the high polymer/treated clay interaction levels, owing to a plasticizing effect of the low molecular weight organic cations. The XRD results show that the gallery heights have increased by the dynamic melt mixing process. In general, as the processing time increases, property changes are more significant, implying the significant importance of the processing conditions in the structuring of a given nanocomposite system.

ACKNOWLEDGMENTS

The authors are grateful to the Israel Ministry of Science and Culture for partially supporting the nanocomposite project. Thanks are also due to the Chinese Academy of Sciences, Institute of Physics, for providing the XRD results.

REFERENCES

1. R. A. Vaia, H. Ishii and E. P. Giannelis, *Chem. Mater.*, **5**, 1694 (1993).
2. R. A. Vaia, B. B. Sauer, O. K. Tse and E. P. Giannelis, *J. Polym. Sci., Part B: Polym. Phys.*, **35**, 59 (1997).
3. N. Hasegawa, M. Kawasumi, M. Kato, Usuki and A. Okada, *J. Appl. Polym. Sci.*, **67**, 87 (1998).
4. R. A. Vaia, K. D. Jandt, E. J. Kramer and E. P. Giannelis, *Chem. Mater.*, **8**, 2628 (1996).
5. P. Reichert, J. Kressler, R. Thomann, R. Mulhaupt and G. Stoppelmann, *Acta Polymer*, **49**, 116 (1998).
6. P. B. Messersmith and E. P. Giannelis, *J. Polym. Sci., Part A: Polym. Chem.*, **33**, 1047 (1995).
7. R. A. Vaia, S. Vasudevan, W. Krawiec, L. G. Scanlon and E. P. Giannelis, *Adv. Mater.*, **7**, 154 (1995).
8. A. Usuki, M. Kato, A. Okada and T. Kurauchi, *J. Appl. Polym. Sci.*, **63**, 137 (1997).
9. Y. Kurokawa, H. Yashuda and A. Oya, *J. Mater. Sci., Lett.*, **15**, 1481 (1996).
10. A. Okada and A. Usuki, *Mater. Sci. Eng.*, **C3**, 109 (1995).
11. C. Zilg, R. Thomann, R. Mulhaupt and J. Finter, *Adv. Mater.*, **1**, 49 (1999).
12. N. Hasegawa, H. Okamoto, M. Kawasumi and A. Usuki, *J. Appl. Polym. Sci.*, **74**, 3359 (1999).
13. X. Kornmann, H. Lindberg and L. A. Berlund, *ANTEC' 99*, 1623 (1999).
14. S. Wang, C. Long, X. Wang, Q. Li and Z. Qi, *J. Appl. Polym. Sci.*, **69**, 1557 (1998).
15. E. P. Giannelis, *Adv. Mater.*, **8**, 29 (1996).
16. L. Liu, Z. Qi and X. Zhu, *J. Appl. Polym. Sci.*, **71**, 1133 (1999).
17. X. Kornmann, L. A. Berglund, J. Sterte and E. P. Giannelis, *Polym. Eng. Sci.*, **38**, 1351 (1998).
18. S. S. Bhagawan, D. K. Tripathy, and S. K. De, *J. Appl. Polym. Sci.*, **34**, 1581 (1987).
19. N. Nemirovski and M. Narkis, *Makromol. Chem., Macromol. Symp.*, **76**, 241 (1993).
20. M. Narkis and J. Miltz, *J. Appl. Polym. Sci.*, **12**, 1031 (1968).
21. M. Narkis, M. Zilberman and A. Siegmann, *Polym. Adv. Tech.*, **8**, 525 (1997).
22. J. A. Ratto, D. M. Steeves, E. A. Welsh and B. E. Powell, ANTEC' 99, 1628 (1999).
23. D. C. Lee and L. W. Jang, *J. Appl. Polym. Sci.*, **61**, 1117 (1996).
24. Y. Ke, C. Long and Z. Qi, *J. Appl. Polym. Sci.*, **71**, 1139 (1999).
25. R. Krishnamoorti, R. A. Vaia and E. P. Giannelis, *Chem. Mater.*, **8**, 1728 (1996).
26. K. Iisaka, K. Shibayama, *J. Appl. Polym. Sci.*, **22**, 1321 (1978).
27. I. Galperin, *J. Appl. Polym. Sci.*, **11**, 1475 (1967).
28. D. H. Droste and A. T. DiBenedetto, *J. Appl. Polym. Sci.*, **13**, 2149 (1969).
29. Z. Wang and T. J. Pinnavaia, *Book of Abstracts*, ACS National Meeting, San Francisco (March 2000).